

# 1,3-Disubstituted 4-aminopiperidines as useful tools in the optimization of the 2-aminobenzo[a]quinolizine dipeptidyl peptidase IV inhibitors

Thomas Lübbers,\* Markus Böhringer, Luca Gobbi, Michael Hennig, Daniel Hunziker, Bernd Kuhn, Bernd Löffler, Patrizio Mattei, Robert Narquizian, Jens-Uwe Peters, Yves Ruff, Hans Peter Wessel and Pierre Wyss

Discovery Research, Pharmaceutical Division, F. Hoffmann-La Roche Ltd, CH-4070 Basel, Switzerland

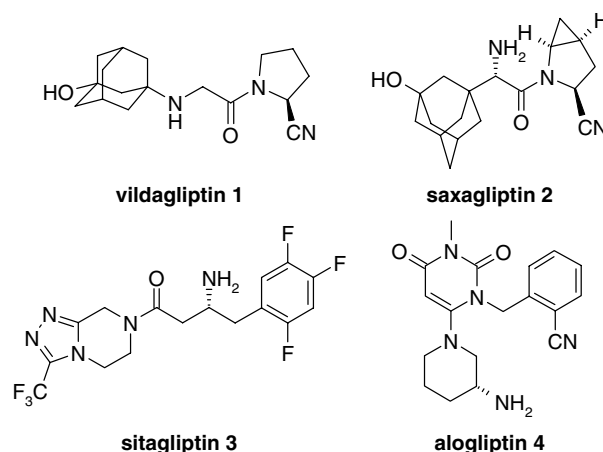
Received 5 February 2007; revised 20 March 2007; accepted 22 March 2007  
Available online 25 March 2007

**Abstract**—In a search for novel DPP-IV inhibitors, 2-aminobenzo[a]quinolizines were identified as submicromolar HTS hits. Due to the difficult synthetic access to this compound class, 1,3-disubstituted 4-aminopiperidines were used as model compounds for optimization. The developed synthetic methodology and the SAR could be transferred to the 2-aminobenzo[a]quinolizine series, leading to highly active DPP-IV inhibitors.

© 2007 Elsevier Ltd. All rights reserved.

The incretin hormone glucagon-like peptide-1 (GLP-1) is released from the gastrointestinal tract in response to nutrient ingestion, and stimulates insulin secretion from the pancreas in a glucose-dependent manner. GLP-1 is degraded by dipeptidyl peptidase IV (DPP-IV), a multifunctional type II transmembrane serine protease which cleaves a dipeptide from the N-terminus of peptide substrates with either proline or alanine at the penultimate position. Once in circulation, GLP-1 has a half-life of only few minutes. Thus, inhibitors of DPP-IV increase levels of GLP-1 and subsequently insulin, and are therefore promising therapeutic agents for the treatment of type 2 diabetes.<sup>1</sup>

There are both covalent and non-covalent inhibitors of DPP-IV in late clinical development (Fig. 1). The cyanopyrrolidines vildagliptin **1** (Novartis, FDA approval filed)<sup>2</sup> and saxagliptin **2** (Bristol-Myers Squibb, phase 3)<sup>3</sup> bind covalently to the active serine in the S1 pocket of DPP-IV, whereas the non-covalent inhibitors sitagliptin **3** (Merck, launched 2006)<sup>4</sup> and alogliptin **4** (Takeda, phase 3)<sup>5</sup> rely entirely on non-covalent protein–ligand



**Figure 1.** Selected clinically studied DPP-IV inhibitors.

interactions and have substituted phenyl groups as ligands for the S1 pocket of DPP-IV.

Clinical trials have proven that DPP-IV inhibitors reduce blood glucose and HbA1c levels in diabetic patients and an excellent safety profile with minimal side effects can be achieved.<sup>6</sup>

In a high throughput screening the 2-aminobenzo[a]quinolizine **5** and the aminopyrimidine derivative **6** were

**Keywords:** Dipeptidyl peptidase IV; DPP-IV inhibitor; 2-Aminobenzo[a]quinolizine.

\* Corresponding author. Tel.: +41 616883095; fax: +41 616886459; e-mail: [thomas.luebbers@roche.com](mailto:thomas.luebbers@roche.com)

identified as inhibitors of DPP-IV (Fig. 2). It turned out that the HTS hits **5** and **6** share a similar structural recognition motif for DPP-IV with sitagliptin **3**, whose structure was not known to us when we performed the research reported in this paper.

The diastereomer **7** of the screening hit **5** had an interesting drug-like profile and was significantly active in an oral glucose tolerance test (OGTT) in fa/fa rats (Table 1).

Particularly, interesting was the 3-butyl substituent in compound **7**, which according to its X-ray complex structure with DPP-IV pointed into the S1 specificity pocket (Fig. 3).<sup>7</sup> The butyl group did not fill the hydrophobic S1 pocket optimally. Synthesis of derivatives with different substituents in 3-position was often cumbersome. Therefore, we looked for a simplified open-chain analogue. The fact that in the 2-aminobenzo[a]quinolizine **8** annulation of a cyclohexyl ring is tolerated suggested 1-substituted 4-amino-3-butylpiperidines **9** as potential DPP-IV inhibitors (Fig. 4).

The 4-aminopiperidines **9** were easily accessible in six steps starting from the commercially available  $\beta$ -ketoester **10** using literature known procedures (Scheme 1).<sup>8</sup> The residue R was introduced through double Hofmann elimination and Michael addition of the amine to the ammonium salt **11**. Oxime-formation and reduction yielded the 4-aminopiperidines **9** as mixtures of

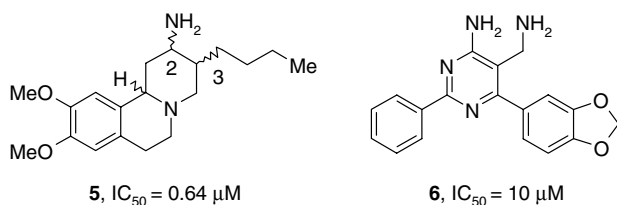
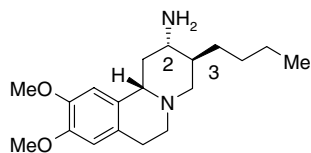


Figure 2. DPP-IV inhibitory activity of selected HTS screening hits.

Table 1. Profile of the 2-aminobenzo[a]quinolizine **7**



DPP-IV $IC_{50}$ (nM)	520
Solubility (mg/L)	>414
log <i>D</i> (pH 7.4)	0.8
Permeation coefficient <i>Pe</i> ( $10^{-6} \text{ cm s}^{-1}$ ) (PAMPA)	2.5
$CL_{\text{micr}}$ (mL/min/mg protein) rat/human	4.7/0.0
$IC_{50}$ CYPs ( $\mu M$ ) (2C9, 2D6, 3A4)	>50
OGTT ( $\Delta_{\text{glucose}}$ , 40 min) (%)	−16

PAMPA, parallel artificial membrane permeation assay;  $CL_{\text{micr}}$ , intrinsic clearance in liver microsome preparations; CYPs, cytochrom P450 enzyme; OGTT, oral glucose tolerance test in fa/fa rats (reduction of glucose levels 40 min after glucose challenge (2 g/kg) compared to non-treated animals; 0.3 mg/kg of **7** given 2 h before glucose challenge).

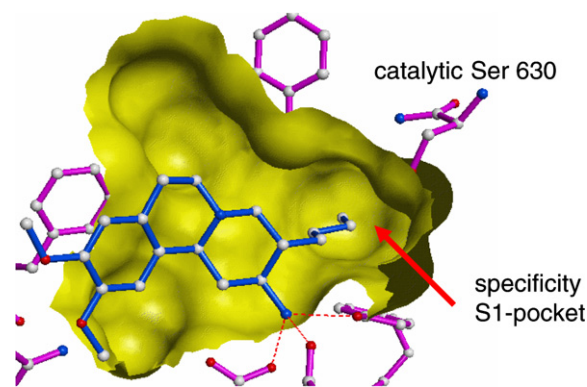


Figure 3. X-ray structure of the binding pocket of the complex of 2-aminobenzo[a]quinolizine **7** with human DPP-IV.

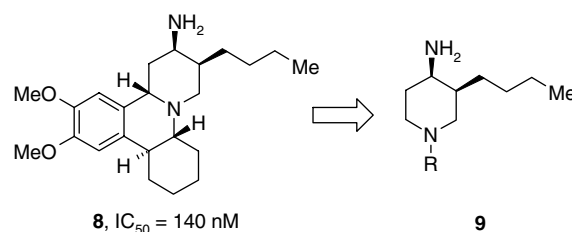
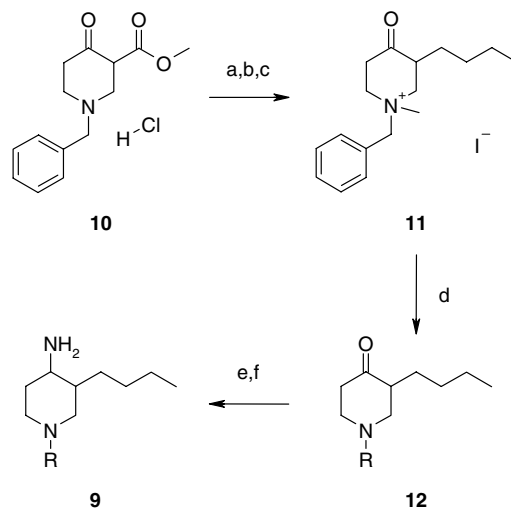


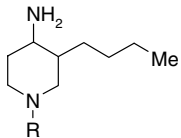
Figure 4. Simplification of the 2-aminobenzo[a]quinolizine structure.



**Scheme 1.** Reagents and conditions: (a) 1.9 equiv BuI, 4.5 equiv  $K_2CO_3$ , 1 equiv *i*-Pr<sub>2</sub>NEt, acetone, reflux, 12 h; (b) 20% aq HCl, reflux, 24 h, 67% over two steps; (c) 1.2 equiv MeI, acetone, rt, 3 h, 78%; (d) 0.8 equiv RNH<sub>2</sub>, 0.13 equiv  $K_2CO_3$ , EtOH, reflux, 3 h, 57–100%; (e) 1.1 equiv  $NH_2OH \cdot HCl$ , 1.1 equiv NaOAc, EtOH, rt, 2 h; (f) Ra–Ni alloy, EtOH, H<sub>2</sub>O, NaOH, rt, 2 h, 23–71% over two steps.

*cis/trans*-diastereomers, which could be often separated by silica gel chromatography.<sup>9</sup>

A phenyl substituent (**9c**) was more active than a cyclohexyl (**9a**) or a benzylic substituent (**9b**) (Table 2).<sup>10</sup> Generally, the *cis*-diastereomer was more potent than the *trans*-diastereomer. Various substitutions with electron-rich (**9j**) as well as electron-poor (**9i**) residues on the aryl moiety were allowed. The most active derivative

**Table 2.** DPP-IV inhibitory activity of 4-aminopiperidine derivatives **9**


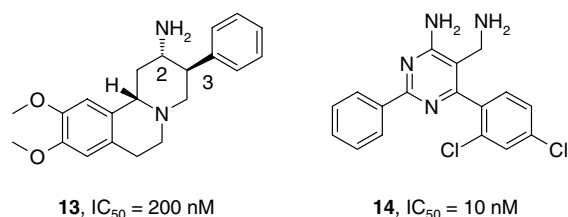
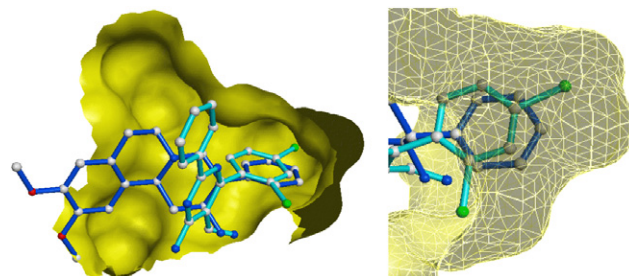
Compound	R <sup>a</sup>	IC <sub>50</sub> (μM)		
		<i>cis</i>	<i>trans</i>	<i>cis/trans</i>
<b>9a</b>	c-Hex			45.2
<b>9b</b>	Ph <sub>2</sub> CH			18.6
<b>9c</b>	Ph	3.5	35.7	
<b>9d</b>	4-PhOPh	6.3	15.0	
<b>9e</b>	4-Tol	5.2	94.7	
<b>9f</b>	3,5-(CF <sub>3</sub> ) <sub>2</sub> -Ph			13.4
<b>9g</b>	3-MeO-5-CF <sub>3</sub> -Ph	2.1		8.4
<b>9h</b>	3-Ph-4-MeO-Ph	5.8	142	
<b>9i</b>	4-Cl-3-CF <sub>3</sub> -Ph	2.8		2.6
<b>9j</b>	3,4-(MeO) <sub>2</sub> -Ph	4.9	26	
<b>9k</b>	3,4,5-(MeO) <sub>3</sub> -Ph	2.3	18.4	
<b>9l</b>	3,4-Cl <sub>2</sub> -Ph	3.3		
<b>9m</b>	2-Naphthyl	1.5	9.4	
<b>9n</b>	5,6,7,8-Tetrahydro-naphthalen-1-yl			13.6
<b>9o</b>	1-Naphthyl			5.3

<sup>a</sup> The numbering refers to the position of the substituent on the corresponding aromatic ring.

was the 2-naphthyl-compound *cis*-**9m**. Because of the relatively flat SAR we decided to keep the more polar 3,4-dimethoxyphenyl group constant and vary the substituent in 3-position.

The phenyl substituted 2-aminobenzo[a]quinolizine **13** exhibited a nice inhibitory activity of 200 nM (Fig. 5). The modeled overlay with the co-crystal structure of DPP-IV with inhibitor **14**,<sup>11</sup> an optimized compound from a previous lead series identified from the HTS hit **6**, clearly showed that a substantial improvement in affinity could be expected by the introduction of the correct substitution pattern on the 3-aryl substituent of the 4-aminopiperidines, respectively, the 2-aminobenzo[a]quinolizines (Fig. 6).

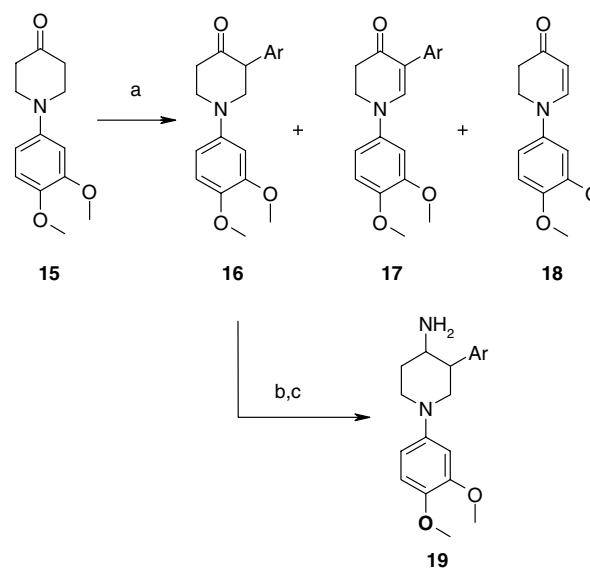
The employed synthetic route to **13** was not generally applicable for the variation of the 3-aryl substituent. Therefore, we decided to study the direct introduction of an aryl substituent into the ketone-precursor. As a model system we choose the 4-aminopiperidines. Several methods such as the direct arylation of the copper-enolate, generated from **15** with LDA and CuCN, with a mixed bis aryl iodonium salt,<sup>12</sup> gave

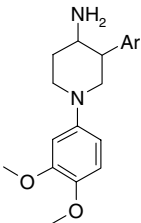
**Figure 5.** DPP-IV inhibitors.**Figure 6.** Modeled overlay of 2-aminobenzo[a]quinolizine **13** with the co-crystal structure of DPP-IV with inhibitor **14** illustrating the asymmetric shape of the S1 pocket.

only low yields (5%). The Pd-catalyzed arylation<sup>13</sup> of **15** was successful, however furnished **16** in low yield (Scheme 2) because of the formation of the dehydro by-products **17** and **18**.

The SAR revealed that a small lipophilic group such as methyl or possibly a halogen substituent in the meta-position of the aromatic residue was favored (Table 3). The toluene derivative **19c** had a IC<sub>50</sub> value of 600 nM combined with a low molecular weight. It was still a diastereomeric mixture.

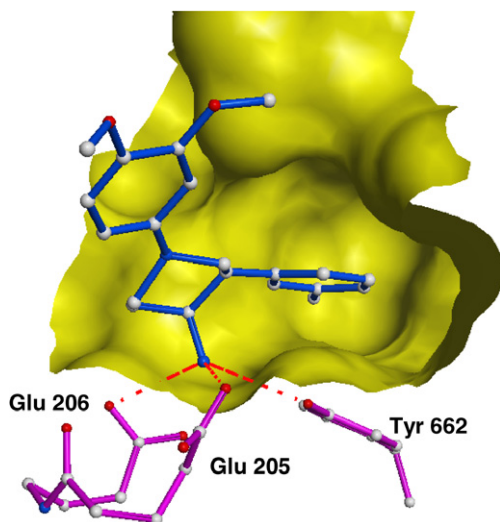
We were able to solve the X-ray complex structure of **19c** with DPP-IV to a resolution of 2.8 Å (Fig. 7).<sup>14</sup> The binding mode revealed clear electron density for the (3*R*,4*S*)-enantiomer of the *cis*-isomer. The protonated primary amine is engaged in the three characteristic hydrogen bonds with Glu 205, Glu 206, and Tyr 662, as seen with other primary amines, such as sitagliptin **3**. The favorable 3-methyl phenyl substituent points into the S1 pocket and perfectly occupies the small hydrophobic niche in the back. Some residual electron density

**Scheme 2.** Reagents and conditions: (a) 1 equiv ArBr, 3 equiv NaO*t*-Bu, 10 mol% Pd(OAc)<sub>2</sub>, 10 mol% Pd*t*-Bu<sub>3</sub>, THF, rt, overnight, 10–27%; (b) 1.1 equiv NH<sub>2</sub>OH·HCl, 1.1 equiv NaOAc, EtOH, rt, 2 h; (c) Ra–Ni alloy, EtOH, H<sub>2</sub>O, NaOH, rt, 2 h, 28–96% over two steps.

**Table 3.** DPP-IV inhibitory activity of 4-aminopiperidine derivatives **19**


Compound	Ar <sup>a</sup>	IC <sub>50</sub> (μM) <i>cis/trans</i>
<b>19a</b>	4-Me-Ph	14.8
<b>19b</b>	3,4-Me <sub>2</sub> -Ph	31.3
<b>19c</b>	3-Me-Ph	0.6
<b>19d</b>	3-MeO-Ph	25.6
<b>19e</b>	2-Pyridyl	8.9

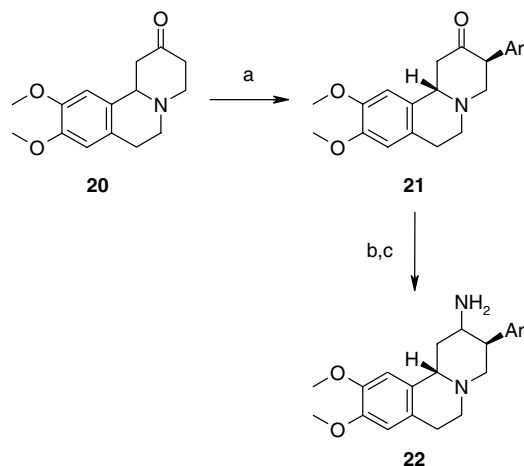
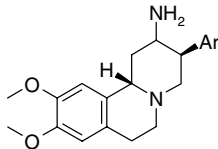
<sup>a</sup> The numbering refers to the position of the substituent on the corresponding aromatic ring.

**Figure 7.** X-ray complex crystal structure of human DPP-IV with compound **19c** (*cis*, (3*R*,4*S*)-enantiomer). Protein residues engaged in hydrogen bonds (dashed red lines) with the ligand are shown.

is, however, seen for a second ligand conformation in which the 3-methyl phenyl substituent is rotated by 180° around the bond connecting the P1 substituent with the piperidine ring.

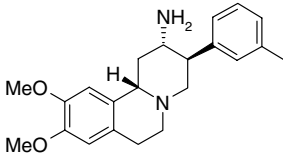
The developed methodology could be nicely transferred to the 2-aminobenzo[a]quinolizines (Scheme 3). Phenyl iodides in general and electron-poor aromatic bromides were not successful in the arylation of the ketone **20**. Aryl chlorides sometimes produced the products **22** in low yields, when the corresponding aryl bromides and iodides failed.

Small lipophilic groups in meta-position, such as methyl or chlorine, were the best substituents, providing compounds with an IC<sub>50</sub> value of 4 nM (*trans*-**22f** and *trans*-**22g**, Table 4). *Trans*-**22f** reduced glucose levels in the oral glucose tolerance test (OGTT) in fa/fa rats by 41% (Table 5) 40 min after the glucose challenge at a

**Scheme 3.** Reagents and conditions: (a) 1 equiv ArBr/Cl, 3 equiv NaOtBu, 10 mol% Pd(OAc)<sub>2</sub>, 10 mol% Pd/Bu<sub>3</sub>, THF, rt, overnight, 11–41%; (b) 1.1 equiv NH<sub>2</sub>OH·HCl, 1.1 equiv NaOAc, EtOH, rt, 2 h; (c) Ra-Ni alloy, EtOH, H<sub>2</sub>O, NaOH, rt, 2 h, 52–73% over two steps.**Table 4.** DPP-IV inhibitory activity of 2-aminobenzo[a]quinolizines **22**


Compound	Ar <sup>a</sup>	IC <sub>50</sub> (nM)		
		<i>cis</i>	<i>trans</i>	<i>cis/trans</i>
<b>22a</b>	Ph	270	200	220
<b>22b</b>	2-Pyridyl	990	1520	
<b>22c</b>	4-Me-Ph	10590	370	
<b>22d</b>	3,4-Me <sub>2</sub> -Ph	9380	3730	
<b>22e</b>	3-MeO-Ph	5130	650	
<b>22f</b>	3-Me-Ph	32	4	13
<b>22g</b>	3-Cl-Ph	50	4	

<sup>a</sup> The numbering refers to the position of the substituent on the corresponding aromatic ring.

**Table 5.** Profile of the 2-aminobenzo[a]quinolizine *trans*-**22f**


DPP-IV IC <sub>50</sub> (nM)	4.6
Solubility (mg/L)	>469
log <i>D</i> (pH 7.4)	1.3
Permeation constant <i>P</i> <sub>e</sub> (10 <sup>−6</sup> cm s <sup>−1</sup> ) (PAMPA)	3.4
CL <sub>micr</sub> (mL/min/mg protein) (rat/human)	1.0/3.0
IC <sub>50</sub> CYPs (μM) (2C9, 2D6, 3A4)	15, 11, >50
OGTT (Δ <sub>glucose</sub> , 40 min) (%)	−41

PAMPA, parallel artificial membrane permeation assay; CL<sub>micr</sub>, intrinsic clearance in liver microsome preparations; CYPs, cytochrom P450 enzyme; OGTT, oral glucose tolerance test in fa/fa rats (reduction of glucose levels 40 min after glucose challenge (2 g/kg) compared to non-treated animals; 0.3 mg/kg of **22f** given 2 h before glucose challenge).

dose of 0.3 mg/kg (applied 120 min before glucose challenge).

In summary, we describe a novel series of 4-aminopiperidine DPP-IV inhibitors. A methodology for the introduction of 3-aryl substituents could be developed. An aromatic residue with a small lipophilic group in meta-position yielded the most active inhibitors. The developed SAR and the synthetic procedures could be applied to the 2-aminobenzo[a]quinazoline series, leading to highly active DPP-IV inhibitors, with *trans*-**22f** and **g** as the best compounds (Table 4).

### References and notes

- Drucker, D. J.; Nauk, M. A. *Lancet* **2006**, *368*, 1696.
- (a) Villhauer, E. B.; Brinkman, J. A.; Naderi, G. B.; Burkey, B. F.; Dunning, B. E.; Prasad, K.; Mangold, B. L.; Russell, M. E.; Hughes, T. E. *J. Med. Chem.* **2003**, *46*, 2774; (b) Barlocco, D. *Curr. Opin. Invest. Drugs* **2004**, *5*, 1094.
- Augeri, D. J.; Robl, J. A.; Betebenner, D. A.; Magnin, D. R.; Khanna, A.; Robertson, J. G.; Wang, A.; Simpkins, L. M.; Taunk, P.; Huang, Q.; Han, S.-P.; Abboa-Offei, B.; Cap, M.; Xin, L.; Tao, L.; Tozzo, E.; Welzel, G. E.; Egan, D. M.; Marcinkeviciene, J.; Chang, S. Y.; Biller, S. A.; Kirby, M. S.; Parker, R. A.; Hamann, L. G. *J. Med. Chem.* **2005**, *48*, 5025.
- (a) Kim, D.; Wang, L.; Beconi, M.; Eiermann, G. J.; Fisher, M. H.; He, H.; Hickey, G. J.; Kowalchick, J. E.; Leiting, B.; Lyons, K.; Marsilio, F.; McCann, M. E.; Patel, R. A.; Petrov, A.; Scain, G.; Patel, S. B.; Roy, R. S.; Wu, J. K.; Wyvratt, M. J.; Zhang, B. B.; Zhu, L.; Thornberry, N. A.; Weber, A. E. *J. Med. Chem.* **2005**, *48*, 141; (b) Deacon, C. F. *Curr. Opin. Invest. Drugs* **2005**, *6*, 419.
- Gwaltney, S. L.; Aertgeerts, K.; Feng, J.; Kaldor, S. W.; Kassel, D. B.; Manuel, M.; Navre, M.; Prasad, G. S.; Shi, L.; Skene, R. J.; Stafford, J. A.; Wallace, M.; Xu, R.; Ye, S.; Zhang, Z.; Webb, D. R. *Abstracts of Papers*, 231st National Meeting of the American Chemical Society, Atlanta, GA, March 26–30, 2006.
- von Geldern, T. W.; Trevillyan, J. M. *Drug Dev. Res.* **2006**, *67*, 627.
- Hunziker, D.; Hennig, M.; Peters, J.-U. *Curr. Top. Med. Chem.* **2005**, *5*, 1623.
- (a) Tortolani, D. R.; Poss, M. A. *Org. Lett.* **1999**, *1*, 1261; (b) Bonjoch, J.; Linares, A.; Guardi, M. *Heterocycles* **1987**, *26*, 2165.
- All new compounds were characterized by  $^1\text{H}$  NMR and MS prior to submission for biological evaluation. For detailed synthetic procedures, see (a) Boehringer, M.; Hunziker, D.; Kuhn, B.; Loeffler, B. M.; Luebbers, T.; Ricklin, F. WO2006066747; (b) Boehringer, M.; Kuhn, B.; Luebbers, T.; Mattei, P.; Narquizian, R.; Wessel, H. P. WO2005000846.
- DPP-IV inhibitors were measured for their ability to inhibit DPP-IV mediated cleavage of Ala-Pro-7-amido-4-trifluoromethylcoumarin in a fluorogenic assay. All compounds were measured in triplicate at 5–7 concentrations in the range of 100  $\mu\text{M}$  to 100 pM.  $\text{IC}_{50}$  values were calculated with a nonlinear best fit regression model. All assays were calibrated with NVP-DPP728 as internal standard inhibitor. NVP-DPP728 under the conditions of the assay showed an  $\text{IC}_{50}$  of  $15 \pm 4$  nM ( $M \pm \text{SD}$ ,  $n = 12$ ) at 50  $\mu\text{M}$  substrate concentration and a  $K_i$  of  $11 \pm 3$  nM determined at substrate concentration range of 10–600  $\mu\text{M}$ .  $\text{IC}_{50}$  values of unknown compounds were accepted when the  $\text{IC}_{50}$  ( $x$ ) measured for NVP-DPP728 in the assay was  $11 < x < 19$  nM.
- Peters, J.-U.; Weber, S.; Kritter, S.; Weiss, P.; Wallier, A.; Boehringer, M.; Hennig, M.; Kuhn, B.; Loeffler, B.-M. *Bioorg. Med. Chem. Lett.* **2004**, *14*, 1491.
- Ryan, J. H.; Stang, P. J. *Tetrahedron Lett.* **1997**, *38*, 5061.
- (a) Fox, J. M.; Huang, X.; Chieffi, A.; Buchwald, S. L. *J. Am. Chem. Soc.* **2000**, *122*, 1360; (b) Kawatsura, M.; Hartwig, J. F. *J. Am. Chem. Soc.* **1999**, *121*, 1473.
- The coordinates of the X-ray complex structure of human DPP-IV with compound **19c** were deposited to the Protein Data Bank (PDBid: 2ijd).